J. of Supercritical Fluids 52 (2010) 258–265

Contents lists available at ScienceDirect

The Journal of Supercritical Fluids

journal homepage: www.elsevier.com/locate/supflu

High carbon dioxide solubilities in trihexyltetradecylphosphonium-based ionic liquids

Pedro J. Carvalho[a], Víctor H. Álvarez[b], Isabel M. Marrucho[a], Martín Aznar[b], João A.P. Coutinho[a,*]

[a] CICECO, Departamento de Química, Universidade de Aveiro, 3810-193 Aveiro, Portugal
[b] Faculdade de Engenharia Química, Universidade Estadual de Campinas, 13083-970, Campinas-SP, Brazil

ARTICLE INFO

Article history:
Received 17 November 2009
Received in revised form 29 January 2010
Accepted 1 February 2010

Keywords:
Trihexyltetradecylphosphonium bis(trifluoromethylsulfonyl)imide
Trihexyltetradecylphosphonium chloride
Carbon dioxide
Phase behavior
Supercritical
Experimental
High pressure
Henry's constant

ABSTRACT

Due to the potential of ionic liquids for industrial application in CO_2 capture and gas separation processes, solubility of near or supercritical CO_2 in ionic liquids has been object of extensive research during the last few years. This work studies the solubility of CO_2 in phosphonium-based ionic liquids that, unlike imidazolium-based ILs, have received little attention in spite of their interesting characteristics. This work addresses the study of the gas–liquid equilibrium of two ionic liquids, trihexyltetradecylphosphonium bis(trifluoromethylsulfonyl)imide and trihexyltetradecylphosphonium chloride, in a wide range of temperatures, pressures, showing that phosphonium ionic liquids can dissolve even larger amounts of CO_2 (on a molar fraction basis) than the corresponding imidazolium-based ILs. In particular trihexyltetradecylphosphonium bis(trifluoromethylsulfonyl)imide seems to be the IL with the largest CO_2 sorption capacity reported up to present, revealing the potential of phosphonium-based ILs for CO_2 capture.

A thermodynamic model based on the Peng–Robinson equation of state with the Wong–Sandler mixing rule, using the UNIQUAC model for the activity coefficients, was here adopted to describe the experimental data and for the estimation of the Henry's constants. A universal correlation, for the description of the solubility of CO_2 in ILs previously proposed by us was also applied to the description of the data here measured showing a good agreement with the experimental data.

1. Introduction

The high solubility of CO_2 in ionic liquids has been the object of extensive research during the last few years. Aiming at enhancing sour gases solubility and ultimately replace the hazard volatile organic compounds (VOCs), many researchers have judiciously tailored ionic liquids (ILs) to accomplish such task either through the introduction of fluorinated groups on the IL ions, or by adding basic groups such as amines or acetates [1–15]. With the exception of this last type of ILs, where chemical interactions dominate the sorption mechanism, in most ionic liquids the gas solubility is simply driven by a physical absorption mechanism [11,16,17]. Among the ILs previously reported in the literature the imidazolium-based ionic liquids, especially those with fluorinated anions such as the bis(trifluoromethylsulfonyl)imide, NTf_2, and bis(pentafluoroethyl)trifluorophosphate, pFAP, are the ones with the highest CO_2 solubilities reported [9,15,18].

Despite their attractive characteristics, such as negligible vapor pressures, high thermal stability, large liquidus range, nonflammability, high solvation capacity, compatibility with strong alkaline solutes, stabilizing effect on palladium catalysts, effective media for Heck and Suzuki reactions and their low cost, the phosphonium-based ionic liquids have received surprisingly little attention in the last few years from academia [8,19–26]. Some authors have focused their study on the solubility of alcohols [27], alkanes and alkenes [25,26,28–32], or even on methane [30,31], carbon monoxide [32] or oxygen [30] in phosphonium ILs but few have reported solubilities of carbon dioxide in these ILs [19,24–26,29]. Furthermore, among those only a couple reported CO_2 solubilities under high pressure [19,29]. Ferguson and Scovazzo [25] have shown that imidazolium and phosphonium-based ILs have similar solubilities for several gases, while Anthony and coworkers [26] suggested that the nature of the anion has the most significant influence on the gas solubility. Hutchings et al. [8] have reported that, at subcritical temperatures, several phosphonium ionic liquids would completely dissolve as soon as all the CO_2 condensed and that the isopleths for these systems follow the vapor pressure curve of the pure CO_2.

Disregarding academia lack of interest, their properties and low cost have attracted the industry attention [33]. Central Glass Co. Ltd., from Japan, developed pharmaceutical intermediates using phosphonium ionic liquids [33], while Texaco used a "*ruthenium melt catalyst*" dispersed in phosphonium or quaternary ammonium ILs to convert syngas into acetic acid, esters, alcohols and glycol

* Corresponding author. Tel.: +351 234 401 507; fax: +351 234 370 084.
E-mail address: jcoutinho@ua.pt (J.A.P. Coutinho).

0896-8446/$ – see front matter © 2010 Elsevier B.V. All rights reserved.
doi:10.1016/j.supflu.2010.02.002

[34]. Rhone-Poulenc, by other hand, used a tetrabutylphosphonium chloride to estabilize zero-valent palladium catalysts for carbonylation [34] and Eastman Chemical Company used a Lewis basic phosphonium iodide ionic liquid along with a Lewis acid catalyst for the isomeration of 3,4-epoxybut-1-ene to 2,5-dihydrofuran [33].

In the wake of previous works [11,17,18,35], the purpose of the present study is to identify ILs with large CO_2 solubilities and to further explore the mechanism behind the absorption of carbon dioxide by the ionic liquids. For that purpose, trihexyltetradecylphosphonium chloride, [THTDP][Cl], and trihexyltetradecylphosphonium bis(trifluoromethylsulfonyl)imide, [THTDP][NTf_2], ionic liquids were chosen. The structure of the phosphonium cation minimizes any specific interactions between the IL cation and the carbon dioxide. Furthermore, the chloride anion of the [THTDP][Cl] allows also to minimize any anion interaction with the CO_2.

The Peng–Robinson equation of state [36] with the Wong–Sandler/UNIQUAC mixing rule [37], using the UNIQUAC model [38] for the activity coefficients, was used to model the experimental data measured in this work and to estimate the Henry's constants from which the enthalpies and entropies of solvation are derived and used to assess the CO_2 IL interactions.

2. Experimental

2.1. Materials

Two ILs based on the trihexyltetradecylphosphonium cation, trihexyltetradecylphosphonium bis(trifluoromethylsulfonyl)imide, [THTDP][NTf_2] and trihexyltetradecylphosphonium chloride, [THTDP][Cl], were used in this study. All compounds were obtained from Cytec with mass fraction purities higher than 97%. The chloride impurity for [THTDP][NTf_2] was inferior to 0.1%. The purities stated by the supplier, of each ionic liquid, were checked by ^{1}H NMR, ^{13}C NMR and ^{19}F NMR.

The ILs where further purified by washing them with ultra pure water followed by drying under high vacuum (1×10^{-3} Pa) and moderate temperature (353 K) for a period of 48 h. The water used was double-distilled, passed through a reverse osmosis system, and further treated with a MilliQ plus 185 water purification apparatus. It has a resistivity of 18.2 MΩ cm, a TOC smaller than 5 μg L^{-1}, and it is free of particles greater than 0.22 μm. The purities of each ionic liquid were checked by ^{1}H NMR, ^{13}C NMR and ^{19}F NMR after each purification step and the purification was repeated until no impurities were observed in the ILs by NMR analysis. The final purity is estimated to be better than 99%. The final IL water content was determined with a Metrohm 831 Karl Fischer coulometer, indicating a water mass fraction of (67 and 97) $\times 10^{-6}$ for [THTDP][NTf_2] and [THTDP][Cl], respectively.

The carbon dioxide (CO_2) was acquired from Air Liquide with a purity of ≥99.998% and H_2O, O_2, C_nH_m, N_2 and H_2 impurities volume fractions lower than (3, 2, 2, 8 and 0.5) $\times 10^{-6}$, respectively.

2.2. Experimental equipment

The high pressure equilibrium cell used in this work is based on a cell designed by Daridon et al. [19,39–42] using the synthetic method. Both the apparatus and the methodology here followed were fully described in previous works [11,18,35], and shown to be adequate to accurately measure vapor–liquid phase equilibrium in a wide range of pressures and temperatures [11,18,19,35,39–42]. The high pressure equilibrium cell, that can operate up to pressures of 1000 bar and in the (283–373) K temperature range, consists of a horizontal hollow stainless-steel cylinder, closed at one end by a movable piston and at the other end by a sapphire window. This window, along with a second window on the cell wall, through which an optical fiber lights the cell chamber, allows the operator to follow the behavior of the sample with pressure and temperature. The orthogonal positioning of both sapphire windows minimizes the parasitic reflections and improves the observation in comparison to axial lighting. A small magnetic bar placed inside the cell allows the homogenization of the mixture by means of an external magnetic stirrer. The presence of the magnetic stirrer, as well as the cell reduced volume, help to minimize the inertia and temperature gradients within the sample. The cell is thermostatized by circulating a heat-carrier fluid through three flow lines directly connected to the cell. The heat-carrier fluid is thermo-regulated with a temperature stability of ±0.01 K by means of a thermostat bath circulator (Julabo MC). The temperature is measured with a high precision thermometer, Model PN 5207 with an accuracy of 0.01 K, connected to a calibrated platinum resistance inserted inside the cell close to the sample. The pressure is measured by a piezoresistive silicon pressure transducer (Kulite) fixed directly inside the cell to reduce dead volumes, that was previously calibrated and certified by an independent laboratory with IPAC accreditation, following the EN 837-1 standard and with accuracy better than 0.2%.

A fixed amount of IL was introduced inside the cell; its exact mass was determined by weighting, using a high weight/high precision balance with an accuracy of 1 mg (Sartorius). In order to avoid any interference of atmospheric gases during the manipulation, after placing the IL inside the cell, it was kept under vacuum overnight while stirring and heating at 353 K.

The CO_2 was introduced under pressure from an aluminum reservoir tank. Its mass was measured with a precision balance and introduced into the measuring cell by means of a flexible high pressure capillary.

After preparation of a mixture of known composition and the desired temperature at low pressure was reached, the pressure was then slowly increased at constant temperature until the system becomes monophasic. The pressure at which the last bubble disappears represents the equilibrium pressure for the fixed temperature.

The purity of the IL is checked again by NMR at the end of the study to confirm that no degradation takes place during the measurements.

2.3. Thermodynamic modeling

To describe the experimental data measured, the Peng–Robinson equation of state [36] was used in this work,

$$P = \frac{RT}{V - b_m} + \frac{a_m}{V(V + b_m) + b_m(V - b_m)} \tag{1}$$

with the Wong–Sandler mixing rule [37]

$$b_m = \frac{\sum\sum x_i x_j (b - a/RT)_{ij}}{1 - \Sigma x_i a_i / b_i RT - A^E_\infty(x)/\Omega RT} \left(b - \frac{a}{RT}\right)_{ij}$$

$$= \frac{1}{2}[b_i + b_j] - \frac{\sqrt{a_i a_j}}{RT}(1 - k_{ij}) \tag{2}$$

$$a_m = b_m \left(\sum x_i \left[\frac{a_i}{a_j} \right] + \frac{A^E_\infty(x)}{\Omega} \right) \tag{3}$$

where a_m and b_m are the equation of state constants, $\Omega = 0.34657$ for the Peng–Robinson equation, and $A^E_\infty(x)$ is calculated using the UNIQUAC model and assuming that $A^E_\infty(x) \approx A^E_0(x) \approx G^E_0(x)$, being $G^E_0(x)$ the excess Gibbs free energy at low pressure described

Table 1
Bubble point data of the system CO_2 (1) + [THTDP][NTf_2] (2).

x_1	T/K	p/MPa	x_1	T/K	p/MPa	x_1	T/K	p/MPa	x_1	T/K	p/MPa	x_1	T/K	p/MPa
0.169	293.26	0.106	0.205	293.34	0.252	0.308	293.20	0.612	0.421	293.30	1.145	0.504	293.37	1.584
0.169	303.25	0.226	0.205	303.22	0.399	0.308	303.15	0.806	0.421	303.22	1.425	0.504	303.58	1.966
0.169	313.20	0.355	0.205	313.10	0.555	0.308	313.16	1.023	0.421	313.24	1.748	0.504	313.05	2.378
0.169	323.26	0.471	0.205	323.11	0.716	0.308	323.25	1.266	0.421	323.22	2.079	0.504	323.24	2.823
0.169	333.25	0.609	0.205	333.15	0.887	0.308	333.13	1.492	0.421	333.38	2.439	0.504	333.21	3.267
0.169	343.22	0.760	0.205	343.20	1.055	0.308	343.13	1.739	0.421	343.19	2.786	0.504	343.27	3.737
0.169	353.21	0.909	0.205	353.21	1.235	0.308	353.11	1.993	0.421	353.21	3.154	0.504	353.26	4.216
0.169	363.24	1.066	0.205	363.40	1.425	0.308	363.29	2.246	0.421	363.34	3.535	0.504	363.45	4.702
0.601	292.88	2.275	0.702	293.14	3.305	0.806	293.17	4.817	0.822	293.15	5.510	0.830	293.20	7.546
0.601	303.27	2.845	0.702	303.11	4.197	0.806	303.31	6.208	0.822	303.20	7.450	0.830	303.20	9.480
0.601	313.10	3.427	0.702	313.11	4.975	0.806	313.39	7.948	0.822	313.19	9.634	0.830	313.23	11.584
0.601	323.24	4.020	0.702	323.15	5.921	0.806	323.28	10.007	0.822	323.31	12.009	0.830	323.23	13.838
0.601	333.22	4.657	0.702	333.27	6.912	0.806	333.29	12.119	0.822	333.24	14.307	0.830	333.28	16.063
0.601	343.20	5.342	0.702	343.38	7.946	0.806	343.40	14.180	0.822	343.10	16.481	0.830	343.28	18.182
0.601	353.23	5.995	0.702	353.33	8.996	0.806	353.23	16.095	0.822	353.20	18.493	0.830	353.41	20.290
0.601	363.31	6.675	0.702	363.53	10.078	0.806	363.28	17.975	0.822	363.21	20.420	0.830	363.45	22.264
0.840	293.20	12.025	0.850	293.33	18.870	0.860	293.30	26.885	0.870	293.26	44.564	0.879	296.58	72.185
0.840	303.18	12.808	0.850	303.10	18.188	0.860	303.02	24.711	0.870	302.95	34.630	0.879	303.08	49.350
0.840	313.29	14.587	0.850	313.21	18.747	0.860	313.18	23.840	0.870	313.10	30.585	0.879	313.35	39.536
0.840	323.19	16.420	0.850	323.22	20.190	0.860	323.34	24.304	0.870	323.24	29.743	0.879	323.35	36.280
0.840	333.23	18.457	0.850	333.26	21.719	0.860	333.19	25.423	0.870	333.20	30.253	0.879	333.38	35.408
0.840	343.18	20.490	0.850	343.12	23.608	0.860	343.19	26.972	0.870	343.12	31.183	0.879	343.23	35.732
0.840	353.26	22.557	0.850	353.01	25.482	0.860	353.26	28.426	0.870	353.25	32.463	0.879	353.06	36.563
0.840	363.14	24.401	0.850	363.14	27.163	0.860	363.28	30.227	0.870	363.35	33.815	0.879	361.67	37.445

as

$$\frac{G^E}{RT} = \sum_{i=1}^{n} x_i \ln\left(\frac{\Phi_i}{x_i}\right) + \frac{Z}{2}\sum_{i=1}^{n} q_i x_i \ln\frac{\theta_i}{\Phi_i} - \sum_{i=1}^{n} x_i q_i \ln\left[\sum_{j=1}^{n}\theta_j \exp\left(-\frac{\lambda_{ij}-\lambda_{ii}}{q_i RT}\right)\right] \quad (4)$$

with

$$\Phi_i = \frac{x_i r_i}{\sum_j x_j r_j} \quad \text{and} \quad \theta_i = \frac{x_i q_i}{\sum_j x_j q_j} \quad (5)$$

The correlation of the experimental data was carried by the minimization of the objective function, *OF*, for

$$OF = \sum_{i=1}^{N}\left[\frac{P^{cal} - P^{exp}}{\sigma_P}\right]^2 \quad (6)$$

where N is the number of data points, P is the pressure, the superscripts "*exp*" and "*cal*" refers to the experimental and calculated values, respectively, and σ_P is the standard deviation of pressure. The experimental uncertainties in the pressure data were used for σ_P. The minimization method was performed using a genetic algorithm code, implemented and fully explained in Álvarez et al. [43]. The difference between experimental and calculated values was calculated as the average percent deviation, expressed in absolute form, as follows:

$$|\Delta P| = \frac{100}{N}\sum_{i=1}^{N}\left[\frac{|P_i^{cal} - P_i^{exp}|}{P_i^{exp}}\right] \quad (7)$$

Furthermore the proposed model was applied, in the diluted region limit, to determine the Henry's constant for the studied systems.

3. Results and discussion

The solubility of carbon dioxide in the studied ILs was measured for mole fractions ranging from 0.2 to 0.9, in the temperature range 293–363 K and pressures from 0.1 to 72 MPa, as reported in Tables 1 and 2 and depicted in Fig. 1. The temperature increase leads to an increase in the equilibrium pressures and by increasing CO_2 concentration, the equilibrium pressures increase gradually at first, and then rapidly for higher CO_2 contents as a liquid–liquid like region is reached, as also observed previously for other ILs

Table 2
Bubble point data of the system CO_2 (1) + [THTDP][Cl] (2).

x_1	T/K	p/MPa	x_1	T/K	p/MPa	x_1	T/K	p/MPa	x_1	T/K	p/MPa	x_1	T/K	p/MPa
0.119	313.16	0.168	0.164	303.35	0.225	0.200	303.42	0.357	0.305	303.40	0.820	0.400	303.27	2.311
0.119	323.16	0.274	0.164	313.03	0.371	0.200	313.27	0.517	0.305	313.54	1.120	0.400	313.56	2.850
0.119	333.46	0.453	0.164	323.30	0.523	0.200	323.40	0.682	0.305	323.66	1.355	0.400	323.57	3.357
0.119	343.37	0.546	0.164	333.30	0.641	0.200	333.50	0.849	0.305	333.59	1.605	0.400	333.63	3.924
0.119	353.30	0.690	0.164	343.00	0.784	0.200	343.68	1.033	0.305	343.52	1.873	0.400	343.55	4.495
0.119	363.22	0.770	0.164	353.16	0.943	0.200	353.75	1.220	0.305	353.66	2.160	0.400	353.46	5.092
			0.164	363.20	1.089	0.200	363.66	1.397	0.305	363.54	2.440	0.400	363.58	5.692
0.503	303.32	2.311	0.603	303.33	3.417	0.701	303.36	4.987	0.752	303.42	5.998	0.800	302.55	14.995
0.503	313.47	2.850	0.603	313.28	4.135	0.701	313.70	6.130	0.752	313.38	7.503	0.800	313.44	16.310
0.503	323.43	3.357	0.603	323.47	4.924	0.701	323.56	7.314	0.752	323.45	9.328	0.800	323.83	17.595
0.503	333.47	3.924	0.603	333.69	5.760	0.701	333.54	8.658	0.752	333.58	11.307	0.800	333.78	19.295
0.503	343.55	4.495	0.603	343.64	6.586	0.701	343.48	10.018	0.752	343.46	13.226	0.800	343.72	21.108
0.503	353.64	5.092	0.603	353.69	7.457	0.701	353.77	11.461	0.752	353.58	15.138	0.800	353.66	22.815
0.503	363.67	5.692	0.603	363.53	8.330	0.701	363.68	12.821	0.752	363.67	16.927	0.800	363.65	24.570

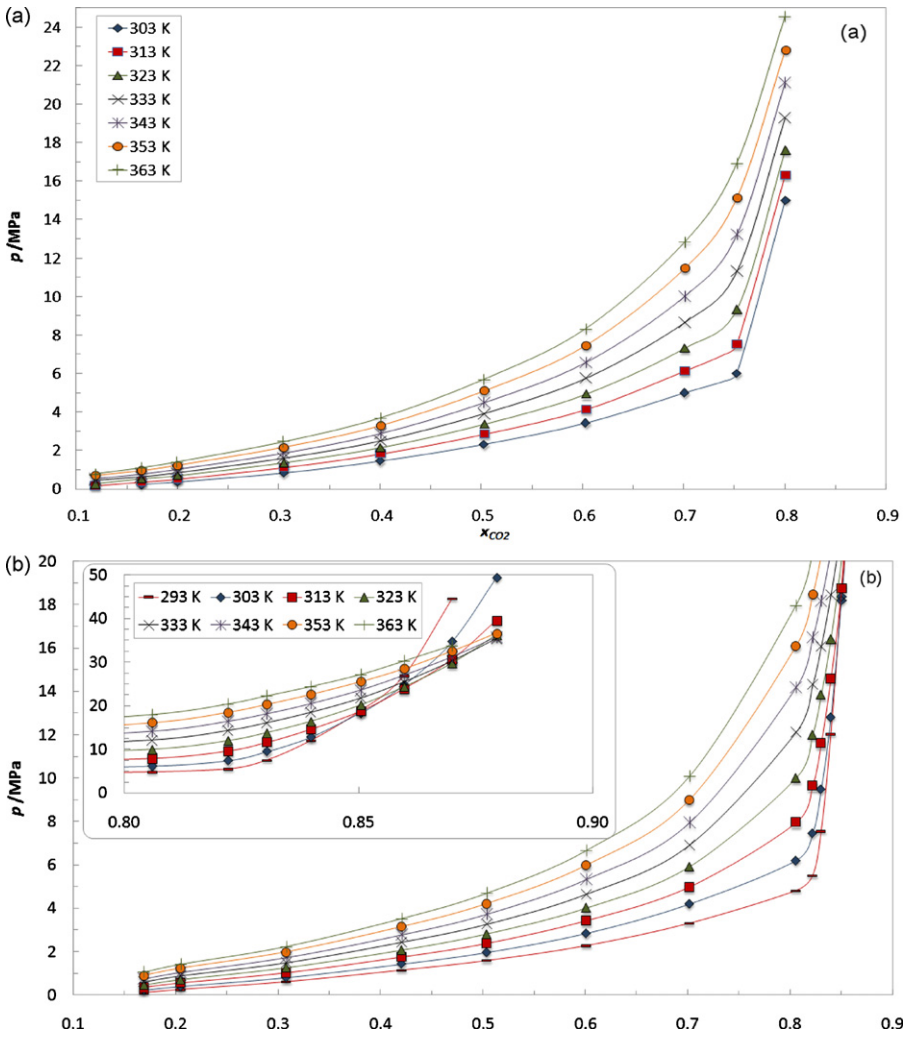

Fig. 1. Pressure–composition diagram of the binary systems: (a) CO_2 + [THTDP][Cl] and (b) CO_2 + [THTDP][NTf_2]. The solid curves are guides for the eye.

[11,18,35]. A singular phenomenon was observed for the system [THTDP][NTf_2] + CO_2 at CO_2 concentrations higher than 0.8. At these conditions the equilibrium pressure changes its behavior and starts to decrease with the temperature increase, as depicted in Figs. 1(b) and 2(b). This unusual behavior, previously observed for the solubility of CO_2 in aqueous solutions of phosphonium-based ILs is related to the liquid–liquid region, as previously noticed [19], and to a change in the relative densities of the phases. At low pressures the IL phase is denser than the CO_2 and dP/dT is positive. At high pressures the CO_2 phase becomes denser than the IL phase and then, as predicted by the Clausius-Clapeyron equation, the dP/dT becomes negative and the solubility increases with temperature.

The solubilities of CO_2 in the ILs studied in this work are among the highest measured up to present. These ILs present identical or higher CO_2 solubilities than those reported for imidazolium-based ILs, with fluorinated anions like the NTf_2 [9,15,44,45] or pFAP [9,15], for which several authors justify the high solubilities as a result of special interactions between the CO_2 and the IL ions. A comparison between the CO_2 solubility in these ILs and in the ILs studied in this work is depicted in Fig. 3.

Hutchings et al. [8] found that for subcritical temperatures several phosphonium ionic liquids, including the [THTDP][Cl] here studied, would completely dissolve in CO_2 as soon as all the CO_2 condensed and that the isopleths for these systems follow the vapor pressure curve of the pure CO_2. In this work we have tried to reproduce the results from Hutchings et al. [8] without success. No significant solubility of phosphonium ionic liquids in near or supercritical CO_2 was observed.

The results of the application of the equation of state to the modeling of the binary systems containing ionic liquids studied in this work are presented in Table 3 for all the experimental data. In the table, *NP* is the number of data points, *T* is the temperature, k_{12}, A_{12} and A_{21} are the interaction parameters of the model, where '1'

Table 3
Temperature-independent interaction parameters and predicted Henry's constant for the studied systems.

[THTDP][NTf_2] + CO_2[a]		[THTDP][Cl] + CO_2[b]	
T/K	H_{12}/MPa	*T*/K	H_{12}/MPa
293.44	1.98		
303.18	2.30	303.27	1.89
313.19	2.64	313.36	2.40
323.24	3.00	323.48	2.99
333.25	3.38	333.55	3.67
343.21	3.76	343.50	4.41
353.22	4.14	353.57	5.21
363.21	4.54	363.54	6.08

[a] $K_{ij} = 0.001116T - 0.2307$, $A_{12} = -2.534 \cdot T + 1867.153$, $A_{21} = 2.490 \cdot T + 351.268$, $|\Delta p|$ (%) = 9.2.
[b] $K_{ij} = 0.00574T - 3.0269$, $A_{12} = 14.331 \cdot T - 3908.572$, $A_{21} = 2.298 \cdot T + 570.848$, $|\Delta p|$ (%) = 9.4.

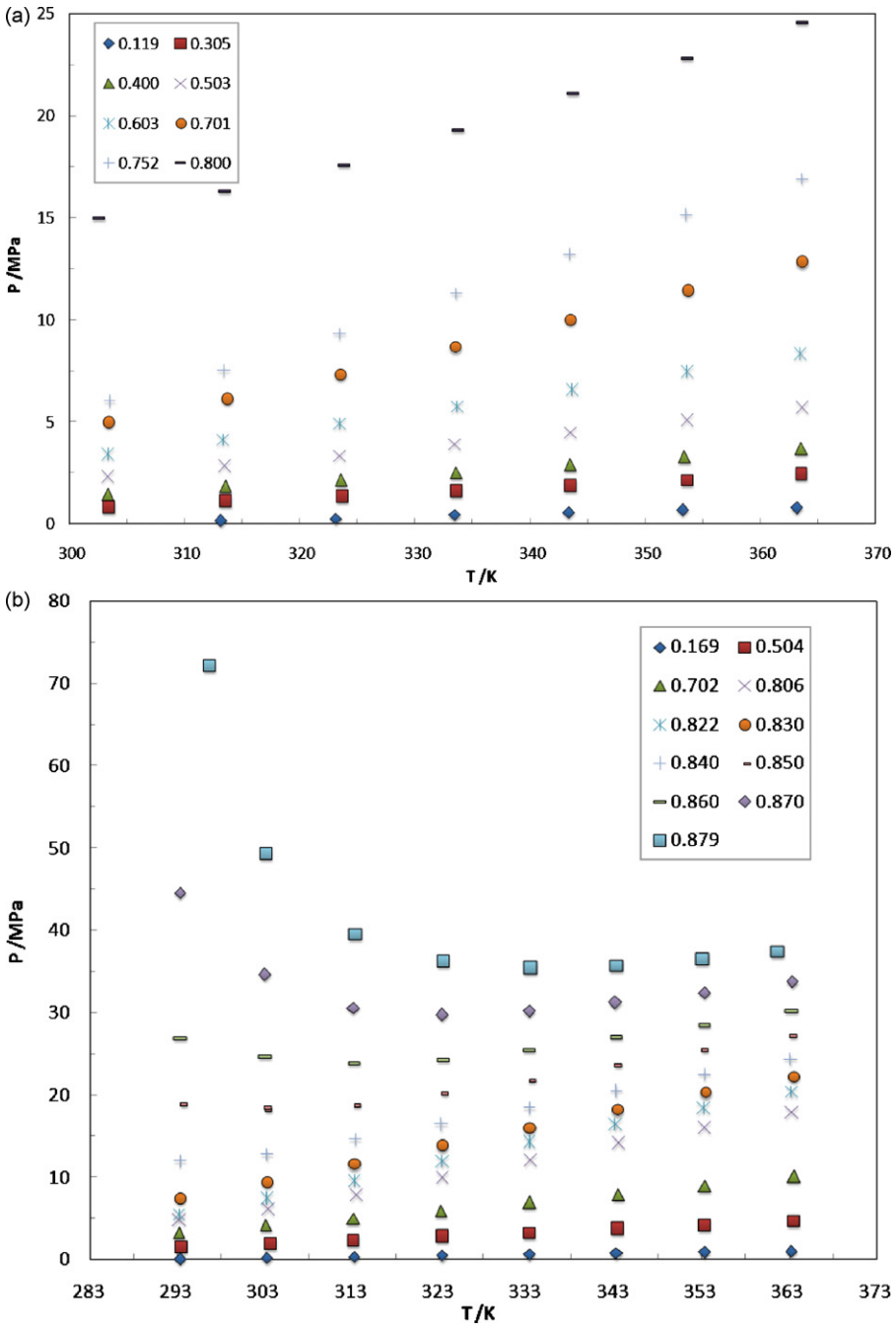

Fig. 2. Pressure–temperature diagram, as function of CO_2 mole fractions, of the binary systems: (a) CO_2 + [THTDP][Cl] and (b) CO_2 + [THTDP][NTf_2].

refers to the CO_2 and '2' for the ionic liquid. This table is divided in sections for each system studied. The properties of the compounds used in the modeling are reported in Table 4. As depicted in Fig. 4, the model provides a good description of the experimental data. The equation of state was then used to estimate the Henry's constant for the studied systems.

Table 4
Properties of the substances used in the modeling.

Compound	T_c/K	P_c/MPa	ω	r	q
CO_2	304.21[a]	7.38[a]	0.2236[a]	3.26[c]	2.38[c]
[THTDP][NTf_2]	1588.22[b]	8.51[b]	0.8801[b]	82.08[c]	52.97[c]
[THTDP][Cl]	1225.80[b]	7.95[b]	0.7698[b]	69.29[c]	44.07[c]

[a] Ref. [47].
[b] Calculated with [48].
[c] Calculated with [49].

The Henry's law relates the amount of gas dissolved in a liquid, at a constant temperature and pressure, to the fugacity of that gas and can be described as

$$H_{12}(T,P) = \lim_{x_1 \to 0} \frac{f_i^L}{x_1} \tag{8}$$

where $H_{12}(T,P)$ is the Henry's constant, x_1 is the mole fraction of gas dissolved in the liquid phase, and f_1^L is the fugacity of the gas in the liquid phase. Eq. (8) is only rigorously valid in the diluted region limit. The Henry's constants for CO_2 in the investigated ILs were estimated by fitting the PR-WS/UNIQUAC model to the experimental data and calculating the limiting slope defined in Eq. (8) as the solubility approaches zero. This approach introduces some uncer-

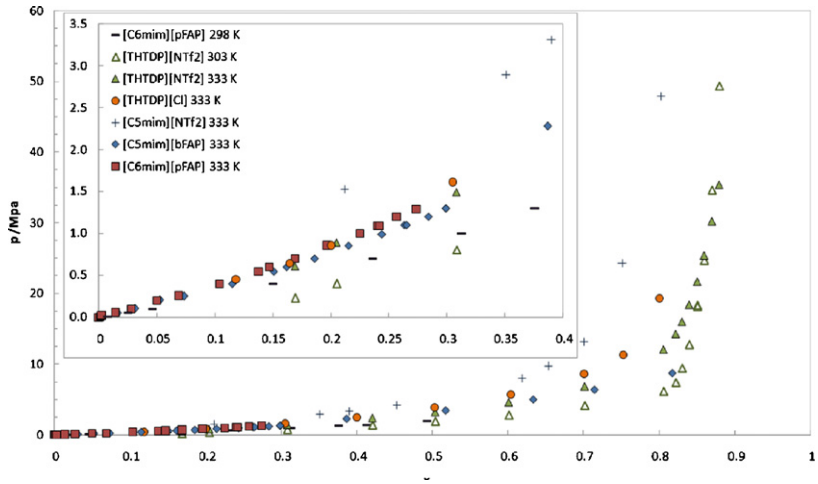

Fig. 3. Pressure–composition diagram of the binary systems: (●) CO_2 + [THTDP][Cl], (▲ , △) CO_2 + [THTDP][NTf_2], (■ , ▬) CO_2 + [C_6mim][pFAP] [9,15], (◆) CO_2 + [C_5mim][pFAP] [9], and (+) CO_2 + [C_5mim][NTf_2] [18].

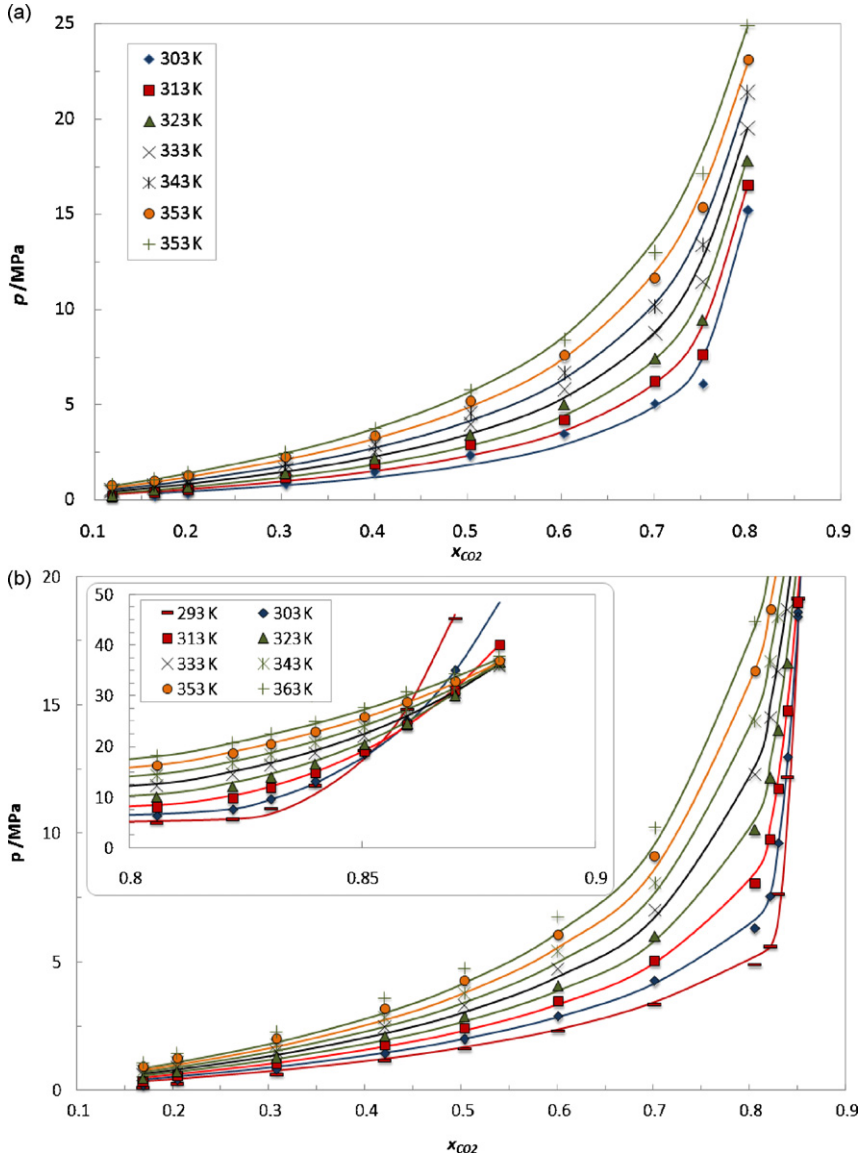

Fig. 4. PTx diagram and modeling for the systems: CO_2 + [THTDP][Cl] (a) and CO_2 + [THTDP][NTf_2] (b). The solid lines represent the calculations with PR-WS/UNIQUAC EoS.

Table 5
Coefficients A and B in Eq. (4) and partial molar enthalpy and partial molar entropy of solvation obtained for CO_2 + ILs systems.

Ionic liquid	A	B	$\lvert\Delta H_{12}\rvert$ (%)	$\Delta_{solv}H$ (kJ mol^{-1})	$\Delta_{solv}S$ (J mol^{-1} K^{-1})	$-T\cdot\Delta_{solv}S\lvert_{T=298\,K}$ (kJ mol^{-1})
[THTDP][NTf$_2$]	−1268.272	5.015	0.65	−10.54	−32.31	9.63
[THTDP][Cl]	−2147.851	7.737	0.84	−17.86	−53.86	16.06

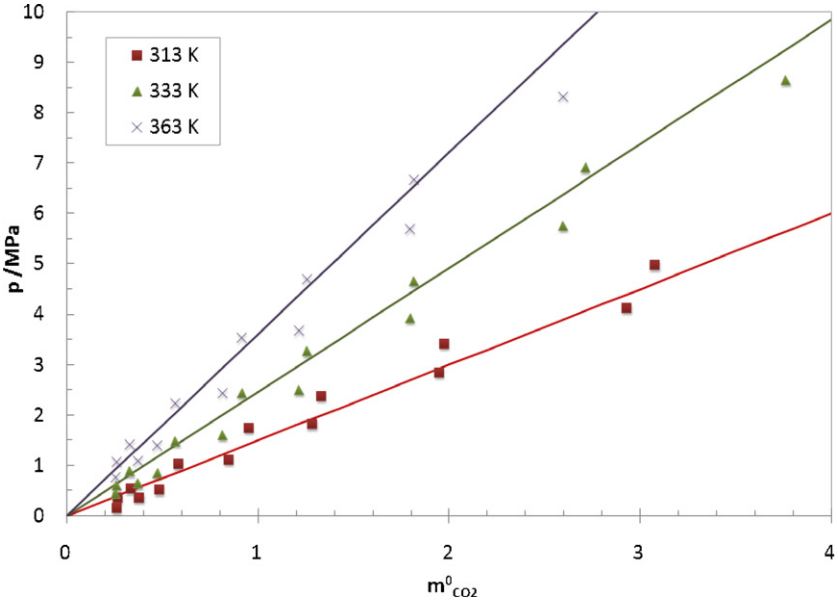

Fig. 5. PTm^0 diagram for the systems CO_2 + ILs. The solid lines represent the universal correlation previously proposed [17].

tainty on the estimated Henry's constants but the values of these constants for the two studied ILs are different enough to allow a discussion of the CO_2 solubility in the two ionic liquids based on these values. The estimated Henry's constants results, reported in Table 3, indicate that Henry's constant slightly decreases (i.e., CO_2 solubility increases) with the temperature.

The results for the Henry's constant of CO_2 in [THTDP][NTf$_2$] and in [THTDP][Cl] were correlated as a function of temperature by an empirical equation of the type:

$$\ln(H_{12}) = A\left(\frac{1}{T}\right) + B \tag{9}$$

where the coefficients A and B are listed in Table 5, together with the Henry's constant average absolute deviations, $|\Delta H_{12}|$, obtained for each ionic liquid.

The effect of temperature on CO_2 solubility can be related to the Gibbs energy, the partial molar entropy and partial molar enthalpy of solvation [46] and can be calculated from an appropriate correlation of Henry's constant:

$$\Delta_{solv}G^\circ = R\cdot T(\ln(H_{12}))_p \tag{10}$$

$$\Delta_{solv}H^\circ = -T^2\left(\frac{\partial\Delta_{solv}G^\circ}{\partial T}\right) = -R\cdot T^2\left(\frac{\partial \ln H_{12}}{\partial T}\right)_p \tag{11}$$

$$\Delta_{solv}S^0 = \frac{\Delta_{solv}H^\circ - \Delta_{solv}G^\circ}{T} = R\cdot T^2\left(\frac{\partial \ln H_{12}}{\partial T}\right) = -R\cdot\ln(H_{12})_p \tag{12}$$

The partial molar enthalpy of solvation gives an indication of the strength of interactions between the gas and the IL, while the partial molar entropy illustrates the amount of ordering present in the gas/IL mixture. The results presented in Table 5 show that the partial molar entropy of CO_2 in [THTDP][Cl] is somewhat higher than in [THTDP][NTf$_2$], indicating a stronger structural solvation interaction for the CO_2/[THTDP][Cl] system. The partial molar enthalpy of solvation of the CO_2 in [THTDP][NTf$_2$] is higher than in [THTDP][Cl], indicating a stronger interaction between the CO_2 and the [THTDP][Cl]. The partial molar enthalpies of solvation observed for these ILs are however similar to those previously reported by us for the imidazolium-based ionic liquids [C$_4$mim][Trifluoroacetate], [C$_4$mim][Dicyanamide] and [C$_4$mim][NTf$_2$] [11,18,35] showing that solvation of CO_2 on phosphonium ILs is similar to what is observed in imidazolium ILs, and driven mainly by entropic effects [17]. Based on this idea, we have proposed a universal correlation for the solubility of CO_2 in ionic liquids [17] that can be described by Eq. (13)

$$p = m_i^0\ e^{(6.8591(-2004.3/T))} \tag{13}$$

where m_i^0 is the carbon dioxide concentration in molality.

In Fig. 5, the predictions obtained are compared to the experimental data measured in this work. As can be seen a good prediction (−7% and 20% for the [THTDP][NTf$_2$] and [THTDP][Cl], respectively) of the experimental data can be obtained using this approach.

4. Conclusions

CO_2 solubility in, trihexyltetradecylphosphonium bis(trifluoromethylsulfonyl)imide and trihexyltetradecylphosphonium chloride was studied in a wide range of temperatures and pressures. It is shown that phosphonium ionic liquids can dissolve even larger amounts of CO_2 (on a molar fraction basis) than the imidazolium-based ILs with the same anion. The solubilities here reported are the largest observed for ionic liquids in absence of chemical interactions. Moreover, an interesting increase of the CO_2 solubility with temperature was observed for these ILs at very high pressures.

A thermodynamic model based on the Peng–Robinson EoS with the Wong–Sandler/UNIQUAC mixing rule was used with success

in the correlation of the measured data. The model provides a good description of the experimental data and the estimation of the Henry's constants for these systems. The enthalpies of solvation derived from the Henry's constants show a lower interaction between the CO_2 and the ILs than previously observed for the imidazolium ionic liquids. A correlation for the solubility of CO_2 in ILs previously proposed by us was applied to the description of the data here measured showing a good agreement with the experimental data measured.

Acknowledgments

The authors are thankful for financial support from Fundação para a Ciência e a Tecnologia (Project PTDC/EQU-FTT/102166/2008) and PhD grant (SFRH/BD/41562/2007) of Pedro J. Carvalho.

The authors would like to acknowledge FAPESP (Fundação de Amparo à Pesquisa do Estado de São Paulo), process #2006/03711-1.

M. Aznar is the recipient of a CNPq fellowship.

The authors are thankful for the ionic liquid samples supplied by Cytec.

References

[1] J.L. Anthony, S.N.V.K. Aki, E.J. Maginn, J.F. Brennecke, Feasibility of using ionic liquids for carbon dioxide capture, Int. J. Environ. Technol. Manage. 4 (2004) 105–115.
[2] J.E Bara, C.J. Gabriel, S. Lessmann, T.K. Carlisle, A. Finotello, D.L. Gin, R.D. Noble, Enhanced CO_2 separation selectivity in oligo(ethylene glycol) functionalized room-temperature ionic liquids, Ind. Eng. Chem. Res. 46 (2007) 5380–5386.
[3] U. Domanska, A. Marciniak, M. Krolikowski, Phase equilibria and modeling of ammonium ionic liquid, C_2NTf_2, solutions, J. Phys. Chem. B 112 (2008) 1218–1225.
[4] A. Finotello, J. Bara, D. Camper, R. Noble, Room-temperature ionic liquids: temperature dependence of gas solubility selectivity, Ind. Eng. Chem. Res. 47 (2007) 3453–3459.
[5] A. Heintz, Recent developments in thermodynamics and thermophysics of non-aqueous mixtures containing ionic liquids. A review, J. Chem. Thermodyn. 37 (2005) 525–535.
[6] G. Hong, J. Jacquemin, M. Deetlefs, C. Hardacre, P. Husson, M. Costa Gomes, Solubility of carbon dioxide and ethane in three ionic liquids based on the bis{(trifluoromethyl)sulfonyl}imide anion, Fluid Phase Equilib. 257 (2007) 27–34.
[7] J. Huang, A. Riisager, R.W. Berg, R. Fehrmann, Tuning ionic liquids for high gas solubility and reversible gas sorption, J. Mol. Catal. A: Chem. 279 (2008) 170–176.
[8] J.W. Hutchings, K.L. Fuller, M.P. Heitz, M.M. Hoffmann, Surprisingly high solubility of the ionic liquid trihexyltetradecylphosphonium chloride in dense carbon dioxide, Green Chem. 7 (2005) 475–478.
[9] M. Muldoon, S. Aki, J. Anderson, J. Dixon, J. Brennecke, Improving carbon dioxide solubility in ionic liquids, J. Phys. Chem. B 111 (2007) 9001–9009.
[10] M.B. Shiflett, D.J. Kasprzak, C.P. Junk, A. Yokozeki, Phase behavior of {carbon dioxide + [bmim][ac]} mixtures, J. Chem. Thermodyn. 40 (2008) 25–31.
[11] P.J. Carvalho, V.H. Álvarez, B. Schröder, A.M. Gil, I.M. Marrucho, M. Aznar, L.M.N.B.F. Santos, J.A.P. Coutinho, Specific solvation interactions of CO_2 on acetate and trifluoroacetate imidazolium based ionic liquids at high pressures, J. Phys. Chem. B 113 (2009) 6803–6812.
[12] E. Bates, R. Mayton, I. Ntai, J. Davis, CO_2 capture by a task-specific ionic liquid, J. Am. Chem. Soc. 124 (2002) 926–927.
[13] X. Yuan, S. Zhang, J. Liu, X. Lu, Solubilities of CO_2 in hydroxyl ammonium ionic liquids at elevated pressures, Fluid Phase Equilib. 257 (2007) 195–200.
[14] J. Sun, S. Zhang, W. Cheng, J. Ren, Hydroxyl-functionalized ionic liquid: a novel efficient catalyst for chemical fixation of CO_2 to cyclic carbonate, Tetrahedron Lett. 49 (2008) 3588–3591.
[15] M.B. Shiflett, A. Yokozeki, Phase behavior of carbon dioxide in ionic liquids: [emim][acetate], [emim][trifluoroacetate], and [emim][acetate] + [emim][trifluoroacetate] mixtures, J. Chem. Eng. Data 54 (2009) 108–114.
[16] A. Yokozeki, M.B. Shiflett, C.P. Junk, L.M. Grieco, T. Foo, Physical and chemical absorptions of carbon dioxide in room-temperature ionic liquids, J. Phys. Chem. B 112 (2008) 16654–16663.
[17] P.J. Carvalho, J.A.P. Coutinho, On the non ideality of CO_2 solutions in ionic liquids and other low volatile solvents, J. Phys. Chem. Lett. (2010), doi:10.1021/jz100009c.
[18] P.J. Carvalho, V.H. Álvarez, J.J.B. Machado, J. Pauly, J. Daridon, I.M. Marrucho, M. Aznar, J.A.P. Coutinho, High pressure phase behavior of carbon dioxide in 1-alkyl-3-methylimidazolium bis(trifluoromethylsulfonyl)imide ionic liquids, J. Supercrit. Fluids 48 (2009) 99–107.
[19] S.P.M. Ventura, J. Pauly, J.L. Daridon, J.A.L. da Silva, I.M. Marrucho, A.M.A. Dias, J.A.P. Coutinho, High pressure solubility data of carbon dioxide in tri-*iso*-butyl(methyl)phosphonium tosylate–water systems, J. Chem. Thermodyn. 40 (2008) 1187–1192.
[20] R.D. Rogers, K.R. Seddon, Ionic liquids—solvents of the future? Science 302 (2003) 792–793.
[21] K.N. Marsh, J.A. Boxall, R. Lichtenthaler, Room temperature ionic liquids and their mixtures – a review, Fluid Phase Equilib. 219 (2004) 93–98.
[22] C. Chiappe, D. Pieraccini, Ionic liquids: solvent properties and organic reactivity, J. Phys. Org. Chem. 18 (2005) 275–297.
[23] M.J. Earle, J.M.S.S. Esperanca, M.A. Gilea, J.N. Canongia Lopes, L.P.N. Rebelo, J.W. Magee, K.R. Seddon, J.A. Widegren, The distillation and volatility of ionic liquids, Nature 439 (2006) 831–834.
[24] S. Zhang, Y. Chen, R. Ren, Y. Zhang, J. Zhang, X. Zhang, Solubility of CO_2 in sulfonate ionic liquids at high pressure, J. Chem. Eng. Data 50 (2005) 230–233.
[25] L. Ferguson, P. Scovazzo, Solubility, diffusivity, and permeability of gases in phosphonium-based room temperature ionic liquids: data and correlations, Ind. Eng. Chem. Res. 46 (2007) 1369–1374.
[26] J. Anthony, J. Anderson, E. Maginn, J. Brennecke, Anion effects on gas solubility in ionic liquids, J. Phys. Chem. B 109 (2005) 6366–6374.
[27] U. Domanska, K. Paduszynski, Phase equilibria study in binary systems (tetra-*n*-butylphosphonium tosylate ionic liquid + 1-alcohol, or benzene, or *n*-alkylbenzene), J. Phys. Chem. B 112 (2008) 11054–11059.
[28] Solubility of adamantane in phosphonium-based ionic liquids, J. Chem. Eng. Data, 55(2010)662–665.
[29] T. Wang, C. Peng, H. Liu, Y. Hu, Description of the PVT behavior of ionic liquids and the solubility of gases in ionic liquids using an equation of state, Fluid Phase Equilib. 250 (2006) 150–157.
[30] R. Condemarin, P. Scovazzo, Gas permeabilities, solubilities, diffusivities, and diffusivity correlations for ammonium-based room temperature ionic liquids with comparison to imidazolium and phosphonium RTIL data, Chem. Eng. J. 147 (2009) 51–57.
[31] D. Morgan, L. Ferguson, P. Scovazzo, Diffusivities of gases in room-temperature ionic liquids: data and correlations obtained using a lag-time technique, Ind. Eng. Chem. Res. 44 (2005) 4815–4823.
[32] J. Anthony, E. Maginn, J. Brennecke, Solubilities and thermodynamic properties of gases in the ionic liquid 1-n-butyl-3-methylimidazolium hexafluorophosphate, J. Phys. Chem. B 106 (2002) 7315–7320.
[33] N.V. Plechkova, K.R. Seddon, Applications of ionic liquids in the chemical industry, Chem. Soc. Rev. 37 (2008) 123–150.
[34] J.F. Jenck, F. Agterberg, M.J. Droescher, Products and processes for a sustainable chemical industry: a review of achievements and prospects, Green Chem. 6 (2004) 544–556.
[35] P.J. Carvalho, V.H. Álvarez, I.M. Marrucho, M. Aznar, J.A.P. Coutinho, High pressure phase behavior of carbon dioxide in 1-butyl-3-methylimidazolium bis(trifluoromethylsulfonyl)imide and 1-butyl-3-methylimidazolium dicyanamide ionic liquids, J. Supercrit. Fluids 50 (2009) 105–111.
[36] D. Peng, D.B. Robinson, A new two-constant equation of state, Ind. Eng. Chem. Fund. 15 (1976) 59–64.
[37] D.S.H. Wong, S.I. Sandler, A theoretically correct mixing rule for cubic equations of state, AIChE J. 38 (1992) 671–680.
[38] D.S. Abrams, J.M. Prausnitz, Statistical thermodynamics of liquid mixtures: a new expression for the excess Gibbs energy of partly or completely miscible systems, AIChE J. 21 (1975) 116–128.
[39] S. Vitu, J.N. Jaubert, J. Pauly, J.L. Daridon, D. Barth, Phase equilibria measurements of CO_2 + methyl cyclopentane and CO_2 + isopropyl cyclohexane binary mixtures at elevated pressures, J. Supercrit. Fluids 44 (2008) 155–163.
[40] J. Pauly, J. Coutinho, J.L. Daridon, High pressure phase equilibria in methane + waxy systems. 1. Methane + heptadecane, Fluid Phase Equilib. 255 (2007) 193–199.
[41] A.M.A. Dias, H. Carrier, J.L. Daridon, J.C. Pamies, L.F. Vega, J.A.P. Coutinho, I.M. Marrucho, Vapor–liquid equilibrium of carbon dioxide–perfluoroalkane mixtures: experimental data and saft modeling, Ind. Eng. Chem. Res. 45 (2006) 2341–2350.
[42] S.P.M. Ventura, J. Pauly, J.L. Daridon, I.M. Marrucho, A.M.A. Dias, J.A.P. Coutinho, High-pressure solubility data of methane in aniline and aqueous aniline systems, J. Chem. Eng. Data 52 (2007) 1100–1102.
[43] V.H. Álvarez, R. Larico, Y. Yanos, M. Aznar, Parameter estimation for VLE calculation by global minimization: genetic algorithm, Braz. J. Chem. Eng. 25 (2008) 409–418.
[44] S. Raeissi, C.J. Peters, Carbon dioxide solubility in the homologous 1-alkyl-3-methylimidazolium bis(trifluoromethylsulfonyl)imide family, J. Chem. Eng. Data 54 (2009) 382–386.
[45] J. Kumelan, Á.P. Kamps, D. Tuma, G. Maurer, Solubility of CO_2 in the ionic liquid [hmim][NTf2], J. Chem. Thermodyn. 38 (2006) 1396–1401.
[46] T.M. Letcher, Developments and Applications in Solubility, Royal Society of Chemistry, 2007.
[47] Diadem Public 1.2, The DIPPR Information and Data Evaluation Manager, 2000.
[48] J. Valderrama, P. Robles, Critical properties, normal boiling temperatures, and acentric factors of fifty ionic liquids, Ind. Eng. Chem. Res. 46 (2007) 1338–1344.
[49] V.H. Álvarez, M. Aznar, Thermodynamic modeling of vapor–liquid equilibrium of binary systems ionic liquid + supercritical {CO_2 or CHF_3} and ionic liquid + hydrocarbons using Peng–Robinson equation of state, J. Chin. Inst. Chem. Eng. 39 (2008) 353–360.